Published in final edited form as:
Biochimie. 2010 February ; 92(2): 171. doi:10.1016/j.biochi.2009.11.006.

A Host-Specific Factor is Necessary for Efficient Folding of the Autotransporter Plasmid-Encoded Toxin

Kathleen N. Nemec[a], **Patricia Scaglione**[a], **Fernando Navarro-García**[b], **Jazmín Huerta**[b], **Suren A. Tatulian**[c], and **Ken Teter**[a,*]

[a] Burnett School of Biomedical Sciences, College of Medicine, University of Central Florida, Orlando, FL 32826, USA

[b] Department of Cell Biology, Cinvestav-Zacatenco, 07000 México, DF, Mexico

[c] Department of Physics, University of Central Florida, Orlando, FL 32816, USA

Abstract

Autotransporters are the most common virulence factors secreted from Gram-negative pathogens. Until recently, autotransporter folding and outer membrane translocation were thought to be self-mediated events that did not require accessory factors. Here, we report that two variants of the autotransporter plasmid-encoded toxin are secreted by a lab strain of *Escherichia coli*. Biophysical analysis and cell-based toxicity assays demonstrated that only one of the two variants was in a folded, active conformation. The misfolded variant was not produced by a pathogenic strain of enteroaggregative *E. coli* and did not result from protein overproduction in the lab strain of *E. coli*. Our data suggest a host-specific factor is required for efficient folding of plasmid-encoded toxin.

Keywords

Autotransporter; Circular dichroism; Plasmid-encoded toxin; Protein folding

1. Introduction

Autotransporters are produced by a range of Gram-negative pathogens [1–3]. The serine protease autotransporters of the *Enterobacteriaceae* (SPATEs) are one subgroup of autotransporters. SPATE proteins are delivered to the extracellular medium by a type V secretion mechanism. Secretion involves the three characteristic domains of an autotransporter: the amino-terminal signal peptide, the mature protein or passenger domain, and the carboxy-terminal β-domain. The signal peptide targets the nascent autotransporter for Sec-dependent transport into the periplasmic space and is then proteolytically removed from the rest of the protein. The β-domain of the remaining proprotein forms a β-barrel pore in the outer membrane which facilitates passenger domain translocation to the extracellular space. Proteolytic processing then releases the SPATE passenger domain into the extracellular milieu.

*Corresponding author. Ken Teter, 12722 Research Parkway, Orlando, FL 32826; Tel: (407) 882-2247; Fax: (407) 384-2062; kteter@mail.ucf.edu.

Although autotransporter folding and outer membrane translocation were originally thought to be self-contained events, chaperones and other accessory factors now appear to play a role in autotransporter biogenesis. Autotransporter translocation, for example, involves the outer membrane protein YaeT/Omp85 [4]. Surface presentation of the IscA autotransporter also appears to involve the assistance of periplasmic chaperones [5–7]. SurA and DegP chaperones have recently been shown to facilitate the outer membrane translocation of SPATE protein EspP [8], but a role for accessory factors in SPATE folding has not yet been established.

The plasmid-encoded toxin (Pet) of enteroaggregative *Escherichia coli* (EAEC) is a 104 kDa SPATE protein. After it is released into the extracellular medium, Pet enters intestinal epithelial cells by clathrin-dependent endocytosis [9]. The internalized toxin then escapes the endomembrane system and cleaves the cytosolic actin-binding protein α-fodrin [10,11]. The resulting disruption to actin architecture and cellular morphology contributes to the pathogen-induced mucosal damage [12].

To determine if Pet folding is a spontaneous process, we purified the toxin from a non-pathogenic HB101 lab strain of *E. coli* and from the pathogenic EAEC. Size exclusion chromatography isolated two variants of Pet from the medium of HB101 *E. coli*. A toxicity assay, circular dichroism (CD), and fluorescence spectroscopy demonstrated that only one of the two variants was in an active, folded conformation. In contrast, EAEC only produced the properly folded variant of Pet. Various levels of protein production did not alter these observations. In vitro denaturation and refolding of the folded Pet from HB101 *E. coli* resulted in the generation of both misfolded and folded variants of the toxin. Our collective data thus indicate that a host-specific factor(s) is required for efficient folding of Pet.

2. Materials and methods

2.1. Toxin purification

To purify Pet from EAEC strain 042ΔPic or an HB101 lab strain of *E. coli* that had been transformed with the pCEFN1 Pet expression vector [13], 37°C overnight cultures were centrifuged at 7,000 × *g* for 15 min. The supernatants were passed through 0.22-μm cellulose acetate membrane filters (Corning, Cambridge, MA), concentrated 100-fold with a 100-kDa cutoff ultrafree centrifugal filter device (Millipore, Bedford, MA), filter sterilized again, and lyophilized for storage at −20°C. Toxin yields from equivalent volumes of culture were determined by Bradford assay (Pierce, Rockford, IL).

2.2. Size exclusion chromatography

Lyophilized Pet was reconstituted in double distilled water and passed through a 2 μm syringe filter before loading onto a HiLoad 16/60 Superdex 75 size exclusion column (Amersham) using an ÄKTA purifier (GE Healthcare). Pet was collected in 1 mL fractions of elution buffer (20 mM Tris pH 7.4 and 25 mM KCl) at a rate of 0.5 mL/min. For the 25°C Pet sample, the toxin was collected in 1.7 mL fractions. Peak fractions were collected and concentrated with 30-kDa molecular weight cut-off filters (Millipore, Bedford, MA). Pet protein concentration was determined by Bradford assay or by $O.D._{280}$ measurement; both methods gave similar results.

2.3. Toxicity assay

10 μg of toxin from Pet peak 1 or Pet peak 2 was added in a final volume of 250 μL to CHO cells seeded in a 24-well plate. The cells were grown at 37°C for 24 hours in Ham's F-12 medium supplemented with 10% fetal bovine serum and penicillin/streptomycin. Toxin-free medium was added to a well of CHO cells for control purposes. Pictures were taken at 10×

magnification with a digital camera mounted on a Zeiss (Gottingen, Germany) Axiovert 25 microscope.

2.4. CD and fluorescence spectroscopy

After the initial fractionation procedure, Pet was dialyzed at 4°C against 20 mM sodium phosphate buffer (pH 7.0) for three one hour exchanges. The final protein concentration was 0.31 mg/mL (peak 1) or 0.45 mg/mL (peak 2). Both CD and fluorescence measurements were performed on the same sample with a 0.4 cm path-length rectangular quartz cuvette and a J-810 spectrofluoropolarimeter (Jasco Corp., Tokyo, Japan). CD spectra were recorded from 190 to 250 nm and averaged from 3 scans. For fluorescence measurements, the sample was excited at 280 nm and the emission spectrum was recorded between 300 to 400 nm. Three scans were collected and averaged to improve the signal-to-noise ratio. Measurements were taken at 18° C.

2.5. Pet denaturation and refolding

After size exclusion chromatography, Pet peaks 1 and 2 were individually denatured in a buffer containing 4 M guanidine hydrochloride (GnHCl), 20 mM dithiothreitol (DTT), 20 mM Tris (pH 7.4), and 150 mM KCl. The concentration of Pet was 200 μg/mL, and a total volume of 1.5 mL was used for the experiment. Denaturation was carried out at room temperature by gently agitating the sample in a 15 mL conical overnight. For toxin refolding, a step-wise decrease in the concentrations of GnHCl and DTT was performed by placing denatured Pet in a Slide-A-Lyzer 20-kDa molecular weight cut-off dialysis cassette (Thermo Scientific, Rockford, IL). The cassette was placed sequentially in 0.5 L of elution buffer containing (i) 2 M GnHCl and 5 mM DTT; (ii) 1M GnHCl and 2.5 mM DTT; (iii) 0.5M GnHCl and 1.5 mM DTT; and (iv) 0.1 M GnHCl and 0.5 mM DTT. All steps were for 2 hours at room temperature, except for the second step which was conducted overnight. A final step involved dialysis against buffer without GnHCl or DTT for 2 hours at room temperature. Refolded Pet was then subjected to size exclusion chromatography as previously stated.

2.6. Computational modeling of SPATE proteins

The structures of Pet and other SPATEs were modeled using hemoglobin protease (PBD_1WXR), a crystallized SPATE [14], as the template. Models were generated with the ESyPred3D online structure predictor [15] located at the ExPASy website (http://www.fundp.ac.be/urbm/bioinfo/esypred/). Space-filling structural models were created with the WebLab Viewer Lite program.

3. Results

3.1. Functional and structural properties of the Pet variants produced by E. coli lab strain HB101

Pet was collected in the concentrated supernatants of *E. coli* HB101 transformed with the pCEFN1 expression vector [13]. By native polyacrylamide gel electrophoresis (PAGE), the purified toxin produced a single well-defined band of approximately 104 kDa molecular mass (Fig. 1A). Surprisingly, subsequent size-exclusion chromatography yielded two distinct elution peaks (Fig. 1B). Both peak fractions contained Pet as assessed by immunoblotting with an anti-Pet polyclonal antibody [16]. We consistently recovered more Pet in fraction 1 than in fraction 2, yet only the second fraction of eluted toxin was active against cultured cells (Fig. 1C).

The functional differences between Pet fractions 1 and 2 might result from structural differences in the two toxin variants. To examine this possibility, we characterized the structural features of Pet fractions 1 and 2 by CD (Fig. 2A) and fluorescence spectroscopy (Fig.

2B). Both methods indeed revealed significantly different structures for Pet fractions 1 and 2. The CD spectrum of Pet fraction 1 exhibited a single minimum at 205 nm, indicating that the secondary structure of Pet fraction 1 was unfolded to a large extent. In contrast, the CD spectrum of Pet fraction 2 exhibited a single minimum around 215 nm characteristic of β-sheet structures [17]. The latter was consistent with the predicted β-helix structure of the toxin passenger domain, a structural motif adopted by most autotransporters [18–21]. The fluorescence spectrum of Pet fraction 1 was red shifted in comparison to Pet fraction 2: fraction 1 exhibited a maximum emission wavelength of 342 nm, while fraction 2 exhibited a maximum emission wavelength of 327 nm. This red shift, which typically results from solvent relaxation, indicated the tryptophan residues of the toxin in fraction 1 were more exposed to water than those of the toxin in fraction 2.

Collectively, our CD and fluorescence data strongly suggested that the secondary structure of Pet in fraction 1 was at least partially disordered and the tertiary structure was loosely packed, whereas the toxin in fraction 2 was correctly folded. This interpretation is further supported by the faster elution rate of the fraction 1 toxin (Fig. 1B), which would be expected for an unfolded protein with a larger gyration radius than a folded variant of the same protein. The lack of cytopathic effect for the fraction 1 toxin also indicated that it was in a misfolded, inactive conformation (Fig. 1C). Native PAGE with 8% (Fig. 1A) or 16% (data not shown) polyacrylamide gels only detected a single species of Pet, so it is unlikely that fraction 1 represented a dimeric or aggregated form of the toxin. The fluorescence data (Fig. 2B) also argue against a toxin aggregate in fraction 1: if Pet fraction 1 was an aggregate, a blue shift of tryptophan fluorescence would likely occur because the surface-exposed tryptophans would be partially secluded from the solvent. Finally, when the toxin in fraction 2 was reapplied to the size-exclusion column, a single elution fraction corresponding to the folded variant of Pet was obtained that generated a CD spectrum characteristic of a folded β-sheet protein (Fig. 3). This control experiment demonstrated that the misfolded variant of Pet did not arise from exposure to the chromatography elution buffer (20 mM Tris pH 7.4, 25 mM KCl) and/or the chromatography process itself. Thus, HB101 *E. coli* produced two variants of Pet that could be distinguished by functional and structural characteristics.

To ensure that the misfolded variant of Pet did not arise from overproduction of the protein, we purified Pet from an *E. coli* HB101 culture that was grown at 25°C. Toxin yield at this temperature was only 5% of the amount obtained at 37°C, yet we again detected two peaks of Pet by size-exclusion chromatography (Fig. 4A). For toxin production at either 37°C or 25°C, peak 1 contained more protein than peak 2. Different proportions of the two peaks were observed at 37°C vs. 25°C, however, and a lower relative yield of Pet peak 2 was obtained from the 25°C sample. The far-UV CD spectrum of Pet peak 1 exhibited a single minimum around 208 nm, which again indicated that the secondary structure of Pet peak 1 was unfolded to a large extent (Fig. 4B). The far-UV CD spectrum of Pet peak 2 exhibited a wide minimum around 215 nm characteristic of β-sheet structures (Fig. 4C). Despite the temperature-dependent difference in the relative amounts of toxin obtained in peaks 1 and 2, these results clearly indicated that two structurally distinct forms of Pet were produced under both high- and low-yield expression conditions. The greater amount of Pet in peak 1 vs. peak 2 from the low-yield 25°C sample further implied that the misfolded Pet variant did not result from overproduction of the protein.

3.2. Denaturation and refolding of Pet

If the proper folding of Pet was difficult to achieve in the absence of accessory factors, then in vitro denaturation and refolding of active Pet would subsequently result in the appearance of both misfolded and folded variants of the toxin. To test this hypothesis, we denatured the peak 2 toxin in GnHCl and allowed it to refold by removing the denaturant with dialysis. Gel

filtration of the refolded toxin isolated two variants of Pet which we call fractions 2.1 and 2.2 (Fig. 5A). Consistent with the original fractionation procedure, more Pet was found in peak 2.1 than in peak 2.2. The CD spectra of these two fractions identified significantly different structures (Fig. 5B). Pet fraction 2.1 had a single minimum around 190 nm, indicating an unfolded protein. Pet fraction 2.2 had a minimum around 212 nm and a weaker molar ellipticity compared to the original fraction 2. This may indicate either an intermediate conformational state of Pet or a combination of conformational populations, including the correctly folded protein; the resolution of CD spectroscopy does not allow distinction between these possibilities. In any event, however, this experiment confirms the hypothesis that the in vitro folding of Pet was an inefficient process in the absence of additional factors.

To determine whether the inactive fraction of Pet could attain its proper conformation, we also denatured the fraction 1 toxin in GnHCl and allowed it to refold by removing the denaturant with dialysis. In contrast to the results obtained with Pet fraction 2, the denaturation/refolding of Pet fraction 1 only produced a single, well-defined peak by size exclusion chromatography (Fig. 5C). The CD spectrum of this fraction demonstrated a minimum around 205 nm, indicative of a largely disordered secondary structure as in the case of the original elution fraction 1 (Fig. 5D). Thus, denaturation/refolding of the inactive Pet variant did not allow some of the misfolded toxin to attain a properly folded state. This indicated the toxin in fraction 1 had entered a terminally misfolded state that could not be reversed by a gradual removal of the chemical denaturants with dialysis, as happened with Pet fraction 2.

3.3. Structural properties of Pet produced by EAEC

The absence of a host-specific chaperone or other factor for Pet folding could explain why a misfolded variant of the toxin was generated by the HB101 lab strain of *E. coli*. To examine this possibility, we purified Pet from an EAEC 042 strain that had been genetically modified to eliminate expression of the Pic autotransporter (EAEC 042ΔPic) [22]. Toxin purification from EAEC 042ΔPic was identical to the procedure used for toxin purification from HB101 *E. coli*, although toxin yield from EAEC 042ΔPic was 50% of the amount obtained from HB101. The final step of toxin purification from EAEC 042ΔPic (i.e., size-exclusion chromatography with the Superdex 75 column) isolated a single eluted peak of Pet (Fig. 6A). The CD spectrum of this sample exhibited a minimum around 214 nm (Fig. 6B), similar to the active Pet in fraction 2 from *E. coli* HB101. The CD spectrum of EAEC-expressed Pet was not exactly identical to fraction 2 from HB101-expressed Pet: there was no positive component at the low wavelength region in the former case, although the lower wavelength region of far-UV CD spectra may be less reliable because of increased light scattering effects. In any case, the prominent single negative component at 214–215 nm indicated a dominant β-sheet conformation in both cases. Thus, in contrast to the HB101 lab strain of *E. coli*, the pathogenic EAEC strain was able to efficiently synthesize the correctly folded Pet protein without producing a detectable amount of the misfolded Pet variant. A straightforward interpretation of this result is that EAEC contains accessory factors that facilitate Pet folding.

4. Discussion

The HB101 lab strain of *E. coli* produced both folded and misfolded variants of Pet, whereas EAEC only produced the properly folded variant of Pet. The two-fold difference in expression levels between HB101 *E. coli* and EAEC was unlikely to cause the observed structural differences between the Pet samples obtained from HB101 *E. coli* vs. EAEC. Furthermore, both folded and misfolded variants of Pet were still produced when a low temperature incubation was used to drastically reduce toxin expression levels in HB101 *E. coli*. These observations strongly suggest that the misfolded variant of Pet does not arise from overproduction of the protein.

Collectively, our data indicate that folding of the SPATE protein Pet is an inefficient process. The release of misfolded Pet from HB101 *E. coli* further indicated that the proper folding of Pet was not required for its secretion. In addition, our work strongly suggests that an accessory factor(s) present in EAEC but not HB101 *E. coli* is necessary for proper folding of the Pet autotransporter. A recent publication [8] describing the role of SurA and DegP chaperones in translocation of the SPATE protein EspP is consistent with the observations reported here. The absence of SurA or DegP function prevented EspP secretion from *E. coli* lab strain MC4100, and in this work we demonstrated that the absence of a host-specific factor prevented efficient folding (but not secretion) of Pet from *E. coli* lab strain HB101. Accumulating evidence thus suggests that both autotransporter folding and secretion are facilitated by accessory factors [4–8].

Previous reports have used Coomassie staining of PAGE gels to assess the purity of Pet [18, 19,23]. However, as shown in Fig. 1A, gel electrophoresis was not sufficient to resolve the two variants of Pet. Chromatography with a high-resolution Superdex 75 column was instead required to detect the two variants of Pet. Likewise, a Superdex 75 column has been used to generate two well-resolved elution peaks for human 5-lipoxygenase, a 78 kDa protein: one fraction represented the iron-containing protein and the other fraction represented the iron-free protein [24]. Other Pet purification procedures have used different columns to isolate the toxin, and these methods apparently did not permit isolation of the misfolded variant of Pet [18,23].

We previously used the Superdex 75 column for Pet purification and noted toxin partitioning into two fractions. That work only used the fraction 2 material for structure/function studies [19]. For this project, we analyzed both Pet fractions and concluded the self-contained event of Pet folding is an error-prone process that results in a substantial pool of terminally misfolded protein. In contrast to the original model of autotransporter biogenesis, it appears that a host-specific factor is required for the efficient folding of Pet. This factor has yet to be identified but is a topic of current investigation.

Our homology-modeled structure of Pet revealed numerous clusters of surface-exposed hydrophobic residues (Fig. 7). This observation could provide a biochemical explanation for Pet misfolding, as its thermodynamically unfavorable surface hydrophobicity would provide a considerable barrier to proper protein folding. Because other SPATEs also appear to contain extended regions of surface hydrophobicity (Fig. 7), the documented inefficiency in Pet folding may represent a common problem for members of the SPATE subfamily.

Acknowledgments

This work was supported by NIH grant R01 AI073783 to K. Teter and a grant from CONACYT, Mexico (60714) to F. Navarro-Garcia.

List of Abbreviations

CD	circular dichroism
DTT	dithiothreitol
EAEC	enteroaggregative *Escherichia coli*
GnHCl	guanidine hydrochloride
Pet	plasmid-encoded toxin
PAGE	polyacrylamide gel electrophoresis
SPATE	serine protease autotransporter of the *Enterobacteriaceae*

References

1. Dautin N, Bernstein HD. Protein secretion in gram-negative bacteria via the autotransporter pathway. Annu Rev Microbiol 2007;61:89–112. [PubMed: 17506669]
2. Henderson IR, Navarro-Garcia F, Desvaux M, Fernandez RC, Ala'Aldeen D. Type V protein secretion pathway: the autotransporter story. Microbiol Mol Biol Rev 2004;68:692–744. [PubMed: 15590781]
3. Yen YT, Kostakioti M, Henderson IR, Stathopoulos C. Common themes and variations in serine protease autotransporters. Trends Microbiol 2008;16:370–379. [PubMed: 18595714]
4. Jain S, Goldberg MB. Requirement for YaeT in the outer membrane assembly of autotransporter proteins. J Bacteriol 2007;189:5393–5398. [PubMed: 17513479]
5. Purdy GE, Hong M, Payne SM. *Shigella flexneri* DegP facilitates IcsA surface expression and is required for efficient intercellular spread. Infect Immun 2002;70:6355–6364. [PubMed: 12379715]
6. Purdy GE, Fisher CR, Payne SM. IcsA surface presentation in *Shigella flexneri* requires the periplasmic chaperones DegP, Skp, and SurA. J Bacteriol 2007;189:5566–5573. [PubMed: 17526712]
7. Wagner JK, Heindl JE, Gray AN, Jain S, Goldberg MB. Contribution of the periplasmic chaperone Skp to efficient presentation of the autotransporter IcsA on the surface of *Shigella flexneri*. J Bacteriol 2009;191:815–821. [PubMed: 19047350]
8. Ruiz-Perez F, Henderson IR, Leyton DL, Rossiter AE, Zhang Y, Nataro JP. Roles of periplasmic chaperone proteins in the biogenesis of serine protease autotransporters of *Enterobacteriaceae*. J Bacteriol 2009;191:6571–6583. [PubMed: 19734313]
9. Navarro-Garcia F, Canizalez-Roman A, Vidal JE, Salazar MI. Intoxication of epithelial cells by plasmid-encoded toxin requires clathrin-mediated endocytosis. Microbiology 2007;153:2828–2838. [PubMed: 17768228]
10. Canizalez-Roman A, Navarro-Garcia F. Fodrin CaM-binding domain cleavage by Pet from enteroaggregative *Escherichia coli* leads to actin cytoskeletal disruption. Mol Microbiol 2003;48:947–958. [PubMed: 12753188]
11. Navarro-Garcia F, Canizalez-Roman A, Burlingame KE, Teter K, Vidal JE. Pet, a non-AB toxin, is transported and translocated into epithelial cells by a retrograde trafficking pathway. Infect Immun 2007;75:2101–2109. [PubMed: 17296748]
12. Henderson IR, Hicks S, Navarro-Garcia F, Elias WP, Philips AD, Nataro JP. Involvement of the enteroaggregative *Escherichia coli* plasmid-encoded toxin in causing human intestinal damage. Infect Immun 1999;67:5338–5344. [PubMed: 10496914]
13. Eslava C, Navarro-Garcia F, Czeczulin JR, Henderson IR, Cravioto A, Nataro JP. Pet, an autotransporter enterotoxin from enteroaggregative *Escherichia coli*. Infect Immun 1998;66:3155–3163. [PubMed: 9632580]
14. Otto BR, Sijbrandi R, Luirink J, et al. Crystal structure of hemoglobin protease, a heme binding autotransporter protein from pathogenic *Escherichia coli*. J Biol Chem 2005;280:17339–17345. [PubMed: 15728184]
15. Lambert C, Leonard N, De Bolle X, Depiereux E. ESyPred3D: Prediction of proteins 3D structures. Bioinformatics 2002;18:1250–1256. [PubMed: 12217917]
16. Navarro-Garcia F, Eslava C, Villaseca JM, et al. In vitro effects of a high-molecular-weight heat-labile enterotoxin from enteroaggregative *Escherichia coli*. Infect Immun 1998;66:3149–3154. [PubMed: 9632579]
17. Sreerama, N.; Woody, RW. Circular dichroism of peptides and proteins. In: Berova, N.; Nakanishi, K.; Woody, RW., editors. Circular Dichroism: Principles and Applications. John Wiley & Sons, Inc; Hoboken: 2000. p. 601-620.
18. Renn JP, Clark PL. A conserved stable core structure in the passenger domain beta-helix of autotransporter virulence proteins. Biopolymers 2008;89:420–427. [PubMed: 18189304]
19. Scaglione P, Nemec KN, Burlingame KE, et al. Structural characteristics of the plasmid-encoded toxin from enteroaggregative *Escherichia coli*. Biochemistry 2008;47:9582–9591. [PubMed: 18702515]
20. Junker M, Schuster CC, McDonnell AV, et al. Pertactin beta-helix folding mechanism suggests common themes for the secretion and folding of autotransporter proteins. Proc Natl Acad Sci USA 2006;103:4918–4923. [PubMed: 16549796]

21. Kajava AV, Steven AC. The turn of the screw: variations of the abundant beta-solenoid motif in passenger domains of Type V secretory proteins. J Struct Biol 2006;155:306–315. [PubMed: 16765057]

22. Henderson IR, Czeczulin J, Eslava C, Noriega F, Nataro JP. Characterization of pic, a secreted protease of *Shigella flexneri* and enteroaggregative *Escherichia coli*. Infect Immun 1999;67:5587–5596. [PubMed: 10531204]

23. Villaseca JM, Navarro-Garcia F, Mendoza-Hernandez G, Nataro JP, Cravioto A, Eslava C. Pet toxin from enteroaggregative *Escherichia coli* produces cellular damage associated with fodrin disruption. Infect Immun 2000;68:5920–5927. [PubMed: 10992503]

24. Pande AH, Moe D, Nemec KN, Qin S, Tan S, Tatulian SA. Modulation of human 5-lipoxygenase activity by membrane lipids. Biochemistry 2004;43:14653–14666. [PubMed: 15544336]

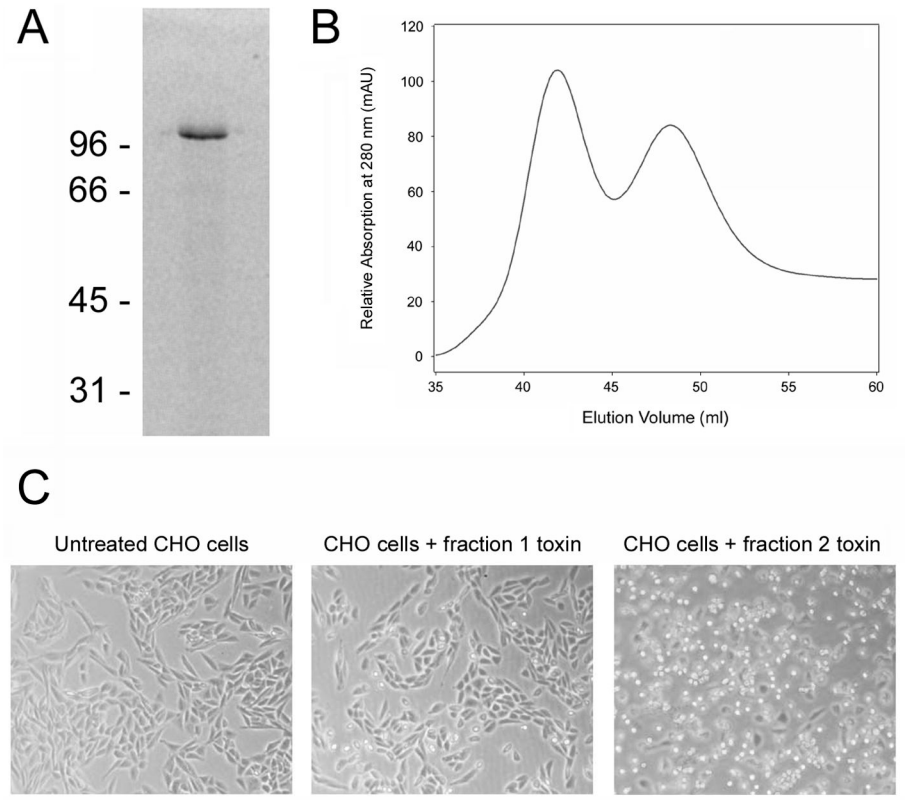

Figure 1.

Isolation of two functionally distinct variants of Pet from *E. coli* HB101. (A): Native gel electrophoresis of Pet prior to size exclusion chromatography. The molecular masses (kDa) of protein standards are indicated. Pet was visualized with Coomassie staining. (B): Elution profile of Pet fractions generated with a HiLoad 16/60 Superdex 75 size exclusion column. (C): Either toxin-free media or Pet-containing media at a final protein concentration of 40 μg/ml was added to CHO cells and incubated overnight at 37°C. Phase contrast images were then taken at 10× magnification. Cell rounding is indicative of productive intoxication.

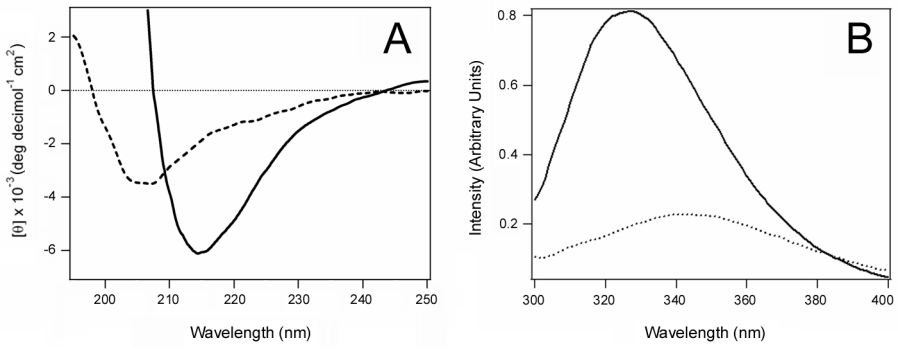

Figure 2.

Structural characteristics of the two Pet variants produced by *E. coli* HB101. (A): Far-UV CD spectra of Pet elution peaks 1 (dashed line) and 2 (solid line) from Fig. 1B. (B): Fluorescence spectra of Pet elution peaks 1 (dashed line) and 2 (solid line) from Fig. 1B.

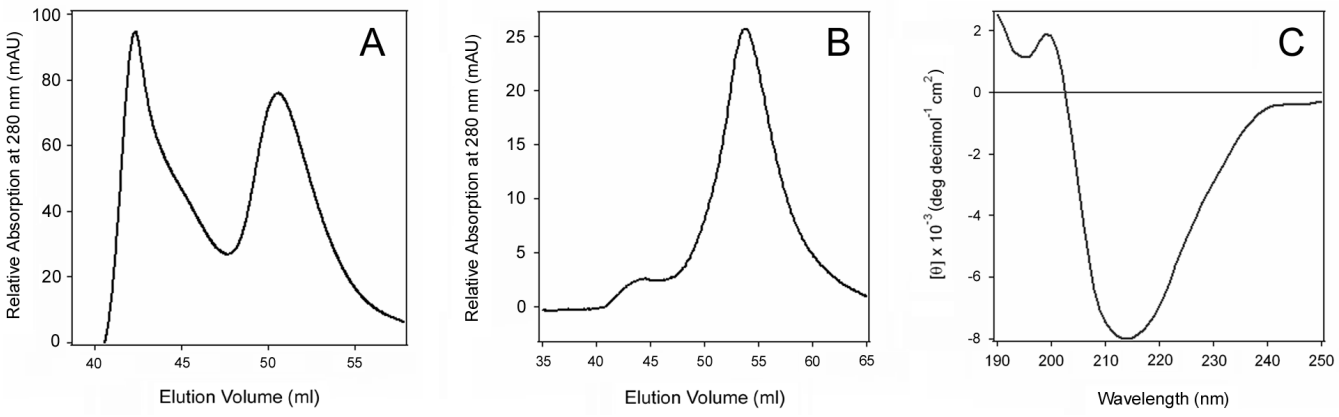

Figure 3.

Stability of Pet after size exclusion chromatography. (A): Pet produced by *E. coli* HB101 was separated into two fractions by size exclusion chromatography. (B): When the toxin in peak 2 was collected and immediately reapplied to the HiLoad 16/60 Superdex 75 size exclusion column, a single peak corresponding to fraction 2 was obtained. (C) Far-UV CD spectrum of the toxin present in the single peak obtained after a second round of chromatography.

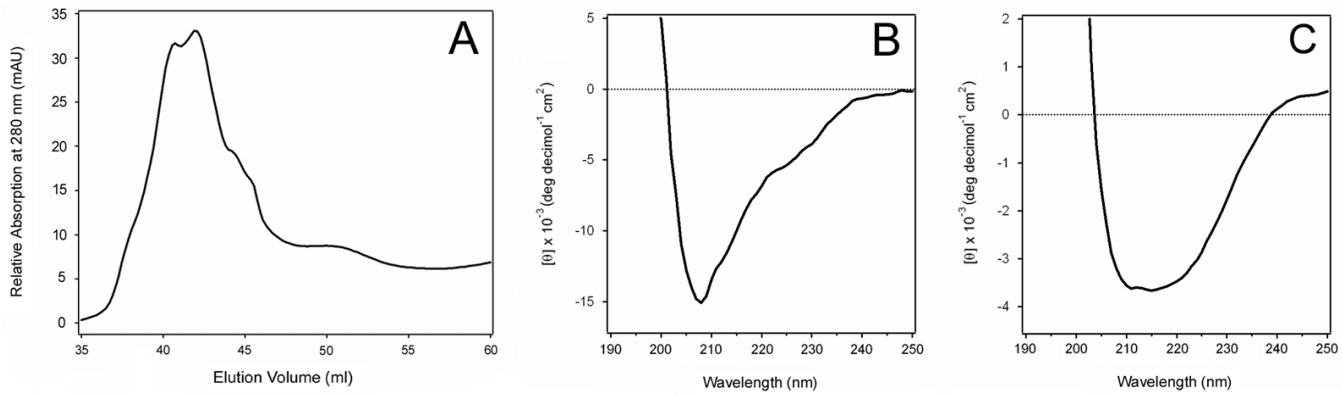

Figure 4.

Structural characteristics of Pet produced by *E. coli* HB101 under suboptimal expression conditions. (A): Pet produced by an *E. coli* HB101 culture grown at 25°C was subjected to size exclusion chromatography with the HiLoad 16/60 Superdex 75 column. At 25°C, toxin yield was 5% of the amount recovered from HB101 cultures grown at 37°C. (B): Far-UV CD spectrum of Pet peak 1 from panel A, collected between 39.3 and 41 ml of elution volume. (B): Far-UV CD spectrum of Pet peak 2 from panel A, collected between 49.5 and 51.2 ml of elution volume.

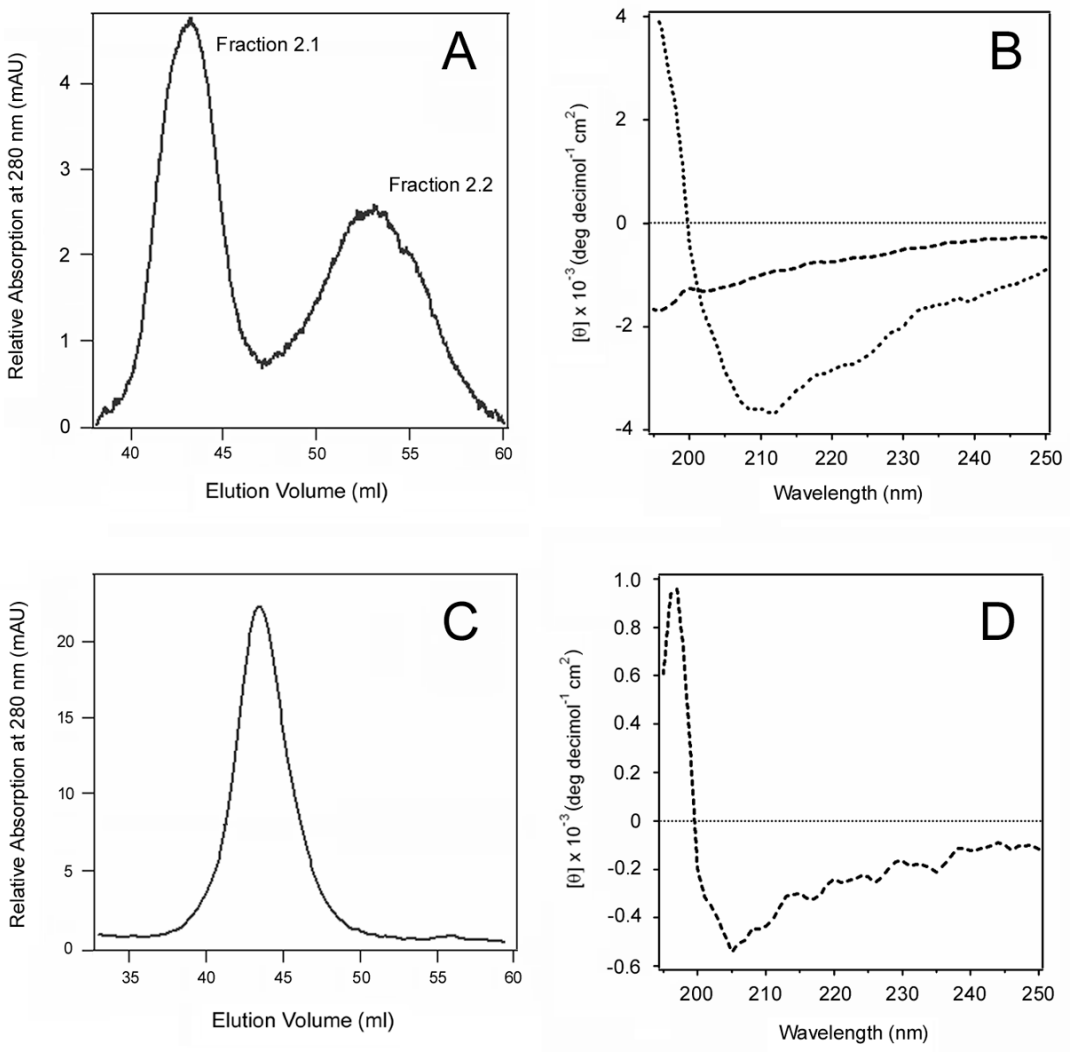

Figure 5.

Structural state of the Pet variants after denaturation and refolding. The peak 2 and peak 1 toxins produced by *E. coli* HB101 were denatured in GnHCl and then allowed to refold by removal of the denaturant with dialysis. (A): The elution profile of Pet peak 2 after denaturation and refolding yielded two peaks, fractions 2.1 and 2.2. (B): Far-UV CD spectra of Pet fractions 2.1 (dashed line) and 2.2 (dotted line). (C): The elution profile of Pet peak 1 after denaturation and refolding. (D): Far-UV CD spectra of Pet peak 1 after denaturation and refolding.

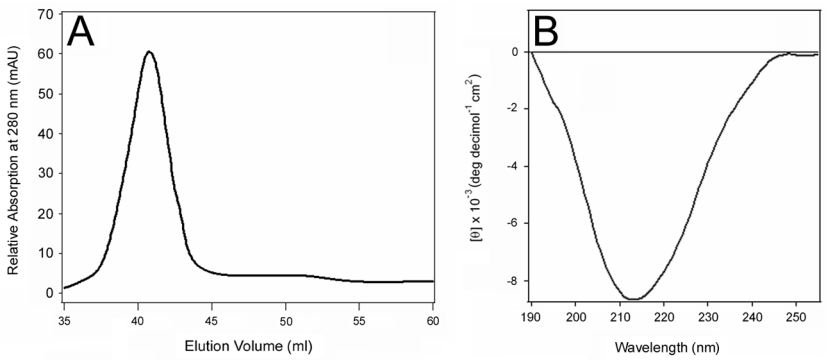

Figure 6.

Isolation of a single Pet variant from EAEC. Pet was purified from a strain of EAEC that had been genetically modified to eliminate the expression of a second autotransporter. (A): Elution profile of Pet generated with a HiLoad 16/60 Superdex 75 size exclusion column. (B): Far-UV CD spectrum of the toxin present in the major peak shown in panel A.

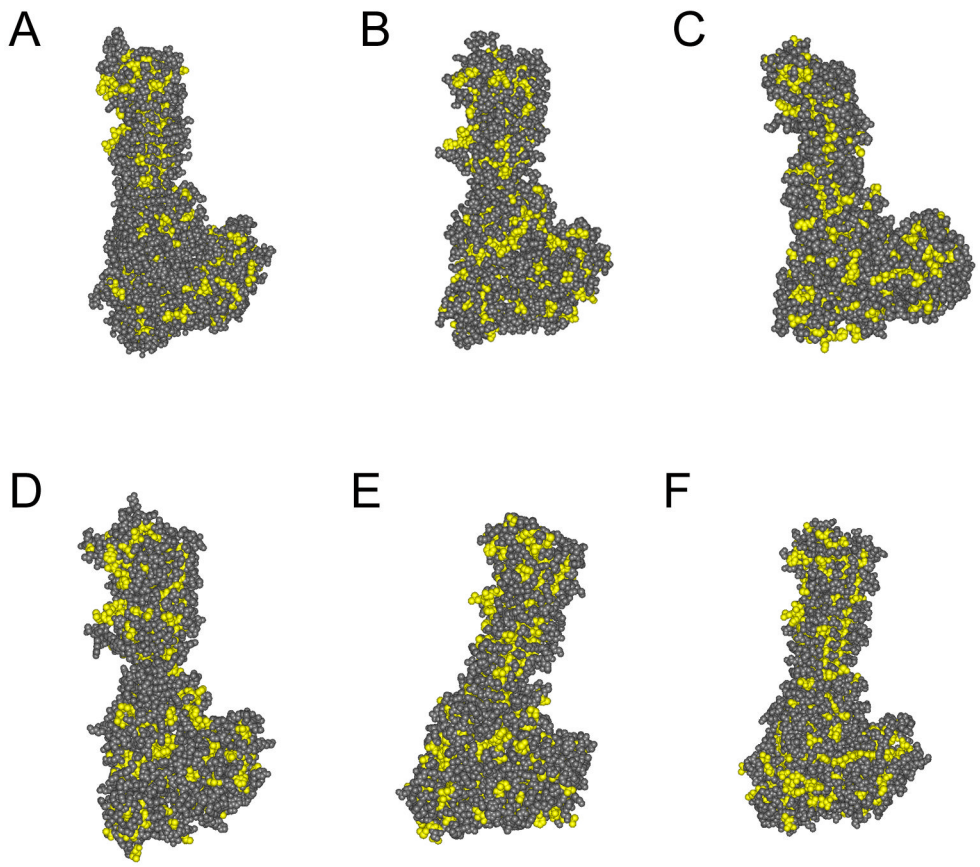

Figure 7.

Homology-modeled structures of SPATE proteins. The structures of Pet and other SPATEs were modeled using hemoglobin protease (PBD_1WXR) as the template. Hydrophobic residues are indicated in yellow. (A) hemoglobin protease; (B) Pet; (C) Sat; (D) EspP; (E) EspC; (F) SepA.